# Perchlorate catalysis reduction by benzalkonium chloride immobilized biomass carbon supported Re-Pd bimetallic cluster particle electrode

Bibo Xu[a,b,c], Yunbo Zhai[a,b,*], Wei Chen[c], Bei Wang[a,b], Tengfei Wang[a,b], Chen Zhang[a,b], Caiting Li[a,b], Guangming Zeng[a,b]

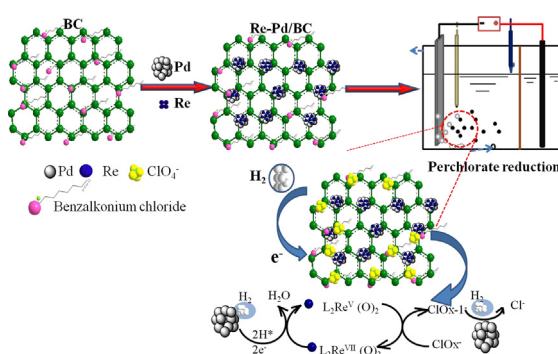[a] College of Environmental Science and Engineering, Hunan University, Changsha 410082, PR China
[b] Key Laboratory of Environmental Biology and Pollution Control (Hunan University), Ministry of Education, Changsha 410082, PR China
[c] Hunan Research Institute for Nonferrous Metals, Changsha 410082, PR China

## HIGHLIGHTS

- Perchlorate could be effectively reduced to chloride by Re-Pd/BC particle electrode.
- The sorption kinetics of Re-Pd/BC could be increased by using benzalkonium chloride.
- Superfluous oxygen, high pH and coexisting nitrate were harmful to reduction.
- Existing form of Re and Pd, H* and current-density played a critical role in reduction.

## GRAPHICAL ABSTRACT



## ARTICLE INFO

## ABSTRACT

This work had demonstrated a novel and high-efficiency perchlorate reduction particle electrode using benzalkonium chloride as dynamics strengthener and coupling with rhenium (Re) and palladium (Pd) nanoparticles (Re-Pd/BC). Perchlorate ions could be rapidly adsorbed in the presence of benzalkonium chloride, facilitating its subsequent reduction on the Re-Pd/BC particle electrode. On the basis of the characterization results and kinetics analysis, a synergistic effect of Re and Pd was observed, perchlorate could be efficiently reduced and completely converted into chlorine in optimized conditions (pH 3.0, anaerobic and current density $20\,mA/cm^2$) and the reduction rate constant of Re-Pd/BC was $0.9451\,L^{-1}\,g_{cat}^{-1}$. The superfluous oxygen in solution could lead to Re-Pd/BC deactivation, and increased current density was beneficial of electro-reduction. The increased pH lead to decrease of reduction efficiency, and the coexisting anion of nitrate could be competed with perchlorate for reduction sites which lead to decrease of reduction rate. Based on the experimental results, it was found that the existing form of Re and Pd on the surface of Re-Pd/BC, the number of atomic H* and current density played an important role in perchlorate electro-reduction process.

## 1. Introduction

Perchlorate $(ClO_4^-)$ is a chemically inert but toxic oxyanion. It is difficult to treated and potentially harmful at very low concentrations [1,2]. In 2011, the United States Environmental Protection Agency (USEPA) announced $ClO_4^-$ in the Contaminants Candidate List (CCL) and

recommended a maximum daily intake for $ClO_4^-$ of 0.7 µg/kg body weight per day [3,4]. To meet this limitation, many treatment technologies have been applied, including chemical reduction, physical adsorption and biological degradation [5–9]. Among these technologies, hydrogenation chemical reduction had proven to be an efficient and clean method to remove perchlorate [8,10]. Liu et al. [11] reported the hydrogenation chemical reduction of perchlorate using a Re $(hoz)_2 - Pd/C$ catalyst. However, hydrogenation chemical reduction of perchlorate needs an external supplied of hydrogen, while transportation and using of hydrogen might be dangerous. In order to avoid using an external supplied of hydrogen, electrochemical production hydrogen was found to be an appropriate approach due to hydrogen supplement itself [12]. The metal ion doped on the cathode electrode exhibited high activities for the hydrogen evolution reaction (HER) by external current [13–15], but the adsorption performance would be evidently decreased. Yao et al. [16] reported an effective electrochemical method to reduce perchlorate to chloride using a two-dimensional electrode reactor with Pd/Pt supported on N-doped activated carbon fiber. The results showed that perchlorate could be effectively removed under the acidic condition, and the perchlorate adsorption capacity would be evidently decreased after metal ions were doped on the carbon material. Hence, it was necessary to improve the adsorption capacity of supporting carbon material. Rhee et al. [17] studied electrochemical reduction perchlorate using a two-dimensional electrode reactor with nano iron supported on porous carbon as electrodes. However, the application of these cathodes for water treatment would be limited due to the low A/V ratio (ratio of the electrode area and solution volume) [18]. It was reported that the treatment efficiency of the target contaminants could be improved by using three-dimensional electrochemical reactor and granular activated carbon (GAC) or modified GAC as particle electrodes compared with a two-dimensional electrode reactor [19,20]. The three-dimensional particle electrodes had more available reactive sites and electrons compared to the conventional two-dimensional electrodes [21]. Re-Pd bimetallic clusters surface of loaded on the carbon material would lead to the decrease of perchlorate adsorption dynamics and capacity. It was not beneficial to perchlorate ions transfer to the carbon material and affect the perchlorate reduction efficiency. The important factor for improved perchlorate reduction efficiency was how to improve the adsorption dynamics and capacity of carbon material, and transfer perchlorate ions to the surface of carbon material rapidly. Although Re-Pd bimetallic catalysts could effectively reduce perchlorate by hydrogen the acidic condition. However, studies on the electro-reduction of perchlorate by Re-Pd bimetallic particle electrode were still limited.

In this study, the Re-Pd bimetallic carbon material strengthened by benzalkonium chloride was synthesized for the first time and evaluated based on its perchlorate reduction efficiency. The main objectives of this study were (1) to characterize the structure characteristics of Re-Pd/BC bimetallic three-dimensional particle electrode; (2) to improve the perchlorate adsorption dynamics of Re-Pd/BC by benzalkonium chloride strengthened; (3) to discuss the different influencing factors of Re-Pd/BC particle electrode for electro-reduction by endogenous hydrogen production; (4) to explain the possible mechanisms involved in the electro-reduction process.

## 2. Experiment section

### 2.1. Material preparation

The biomass carbon material was synthesized according to previous literature [22], which was labeled as CAC crushed and sieved to a particle size fraction of 180–250 µm before it was further treated. Then 1.0 g of CAC was added into the benzalkonium chloride suspension (0.1 wt%) and mixed under stirring for 12 h at 150 rpm. The black solid precipitate (BC) was filtered and washed with deionized water for three times and finally dried at 100 °C for 12 h. The Re-Pd/BC bimetallic catalyst was prepared by a conventional impregnation method. 1.0 g of
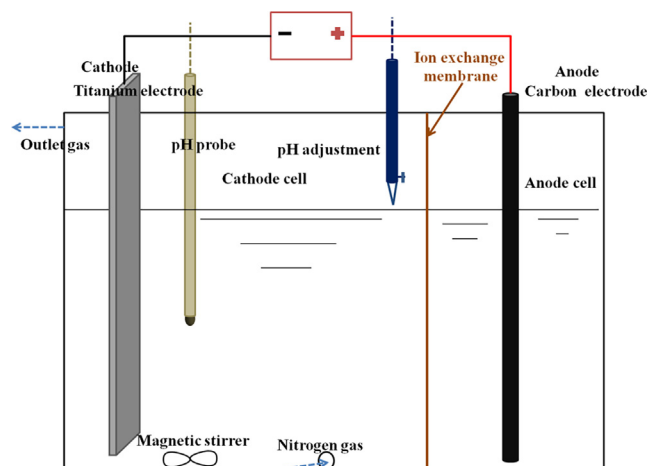


**Fig. 1.** The three-dimensional electrochemical reactor.

BC was immersed in $Pd(NO_3)\cdot 2H_2O$ solution containing 50 mg of Pd and the oscillation at 150 rpm for 10 h. After standing for 2 h, the powders were dried at 110 °C and heated to 250 °C for 1 h under flowing hydrogen before cooled to room temperature (Pd/BC). 1.0 g of Pd/BC was added to $NH_4ReO_4$ solution containing 100 mg of Re; the catalyst suspension was continuously sparged with hydrogen at a rate of 200 mL/min, and HCl was used in pH adjusting (pH3.0). The reaction was carried out for 8 h and ensured complete reductive immobilization of Re onto the Pd/BC material (Re-Pd/BC). The catalyst suspension was then transferred into an anaerobic glovebox chamber (97% $N_2$, 3% $H_2$) and dried at 105 °C (heated sand bath).

### 2.2. Characterizations

The surface area and pore volume distribution of the samples were determined via Brunauer–Emmett–Teller equation, and $N_2$ adsorption–desorption isotherms were measured at −196 °C on Micromeritics ASAP2020 surface area. The morphology images were obtained by using a JEOL JSM-6700F field emission scanning electron microscope operated at 10 kV. X-ray diffraction (XRD) patterns were measured using a powder X-ray diffractometer equipped with JEOLD/ruax2550PC by Cu K radiation (-1.5406 Å) at 40 kV operation voltage and 30 mA current. Raman spectrum was recorded on a Jobin Yvon Laran-010 micro-Raman system Raman spectrometer using a near infrared laser operating at 785 nm with a CCD detector in the range 3000–300 $cm^{-1}$. The samples surface composition and chemical state of elements analyzes were proposed by the X-ray photoelectron spectroscopy (XPS) measurements carried out by the model of ESCALAB 250Xi. Spectra were recorded at constant pass energy of 20 eV and energy step size of 0.1 eV, with Al K$\alpha$ X-ray as source. XPS PEAK 4.1 software was used for fitting the XPS peaks. The zeta potential of the samples was determined by Zetasier Nano ZS (Malvern Instruments Ltd, UK).

### 2.3. Adsorption dynamic experiment

Adsorption dynamic experiment was performed in 150 mL glass conical flasks at room temperature at 150 rpm, and the pH values of solutions were adjusted with 0.1 M NaOH and HCl. 0.1 g of sample was added into 50 mL of $NaClO_4$ solution for different time interval. After the experiment, the suspension was filtered with a 0.45 µm filter membrane and the residue $ClO_4^-$ concentration in suspension was analyzed using Dionex ion chromatograph (IC) systems, equipped with a 25 µL sample loop, a set of 4 × 250 mm AS16 and AG16 columns, a 4 mm ASRS Ultra II suppressor, and an electrical conductivity detector. The suppressor current was 100 mA. The eluent was set to 35 mM KOH.
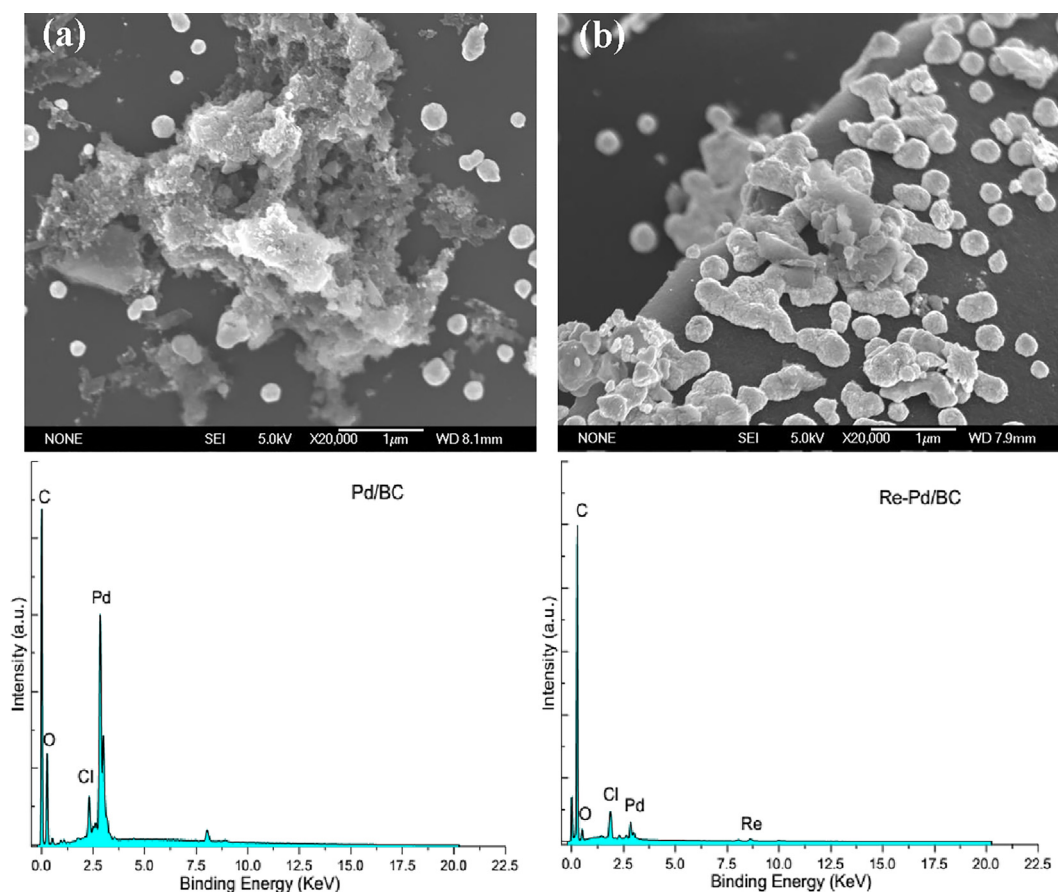
Fig. 2. SEM image of (a) Pd/BC and (b) Re-Pd/BC; EDX spectra of Pd/BC and Re-Pd/BC.
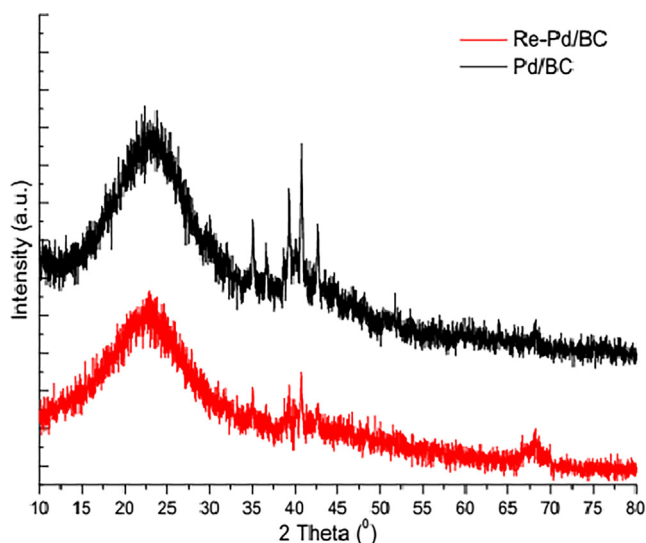


Fig. 3. XRD patterns of Pd/BC and Re-Pd/BC.

All batch experiments were carried out in triplicates and the averages results were recorded.

The adsorption dynamic of $ClO_4^-$ was calculated by Eq. (1).

$$q_t = \frac{(C_i - C_t)V}{m} \tag{1}$$

where $q_t$ (mg/g) was the adsorption amounts of $ClO_4^-$ at equilibrium and at time $t$, $C_i$ was the initial concentration (mg/L) of $ClO_4^-$ in solution, $C_t$ was the residual $ClO_4^-$ concentration at time $t$ (min), $V$ was the volume of solution (L), and $m$ was the dry mass of adsorbent used (g).

### 2.4. Electrochemical catalysis reduction experiments

The three-dimensional electrochemical reactor was shown in Fig. 1. A three-dimensional electrochemical reactor was used for electrochemical reduction experiment. All electrochemical experiments were carried out in a double-chamber electrochemical reactor, and the anode cell (100 mL) and cathode cell (200 mL) were separated by a proton exchange membrane (Nafion117, Dupont). The titanium strip electrode served as the cathode and carbon rod electrode served as the anode. The Re-Pd/BC particles were used as three-dimensional electrode and the

**Table 1**
Surface area, pore volume and elemental composition of CAC, BC, Pd/BC and Re-Pd/BC.

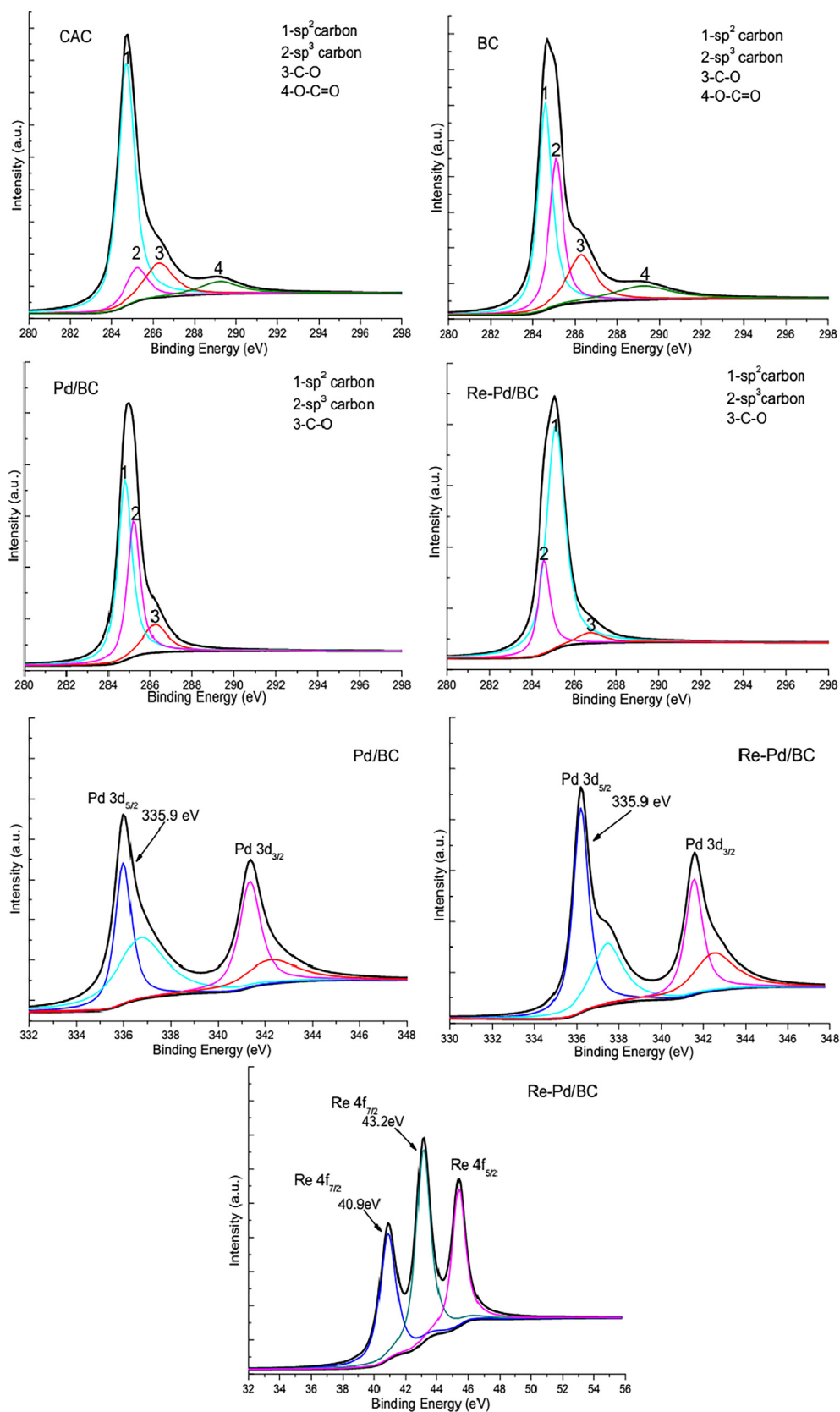| Sample | $S_{BET}$ (m²/g) | Pore volume (cm³/g) | | | C (at.%) | N (at.%) | O (at.%) | Cl (at.%) | Pd (at.%) | Re (at.%) |
|---|---|---|---|---|---|---|---|---|---|---|
| | | Total | Micropore | Mesopore | | | | | | |
| CAC | 1110.35 | 0.605 | 0.133 | 0.472 | 86.5 | 2.9 | 10.6 | – | – | – |
| BC | 794.62 | 0.443 | 0.054 | 0.389 | 88.5 | 2.4 | 7.7 | 1.4 | – | – |
| Pd/BC | 575.06 | 0.331 | 0.023 | 0.308 | 82.2 | 2.6 | 12.0 | 1.3 | 1.9 | – |
| Re-Pd/BC | 379.82 | 0.221 | 0.002 | 0.219 | 82.1 | 2.6 | 11.3 | 1.4 | 1.9 | 0.7 |

**Fig. 4.** C 1s high-resolution XPS spectra of CAC, BC, Pd/BC and Re-Pd/BC; Pd 3d high-resolution XPS spectra of Pd/BC and Re-Pd/BC; Re 4f high-resolution XPS spectra of Re-Pd/BC.
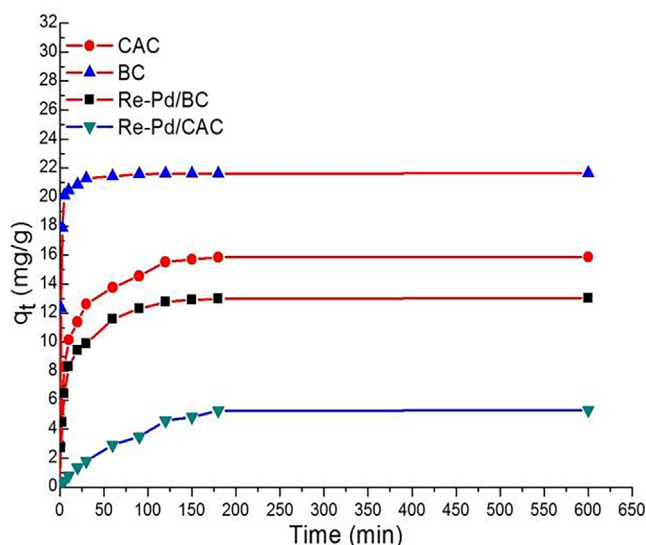
**Fig. 5.** Adsorption kinetics of perchlorate on adsorption materials.

cathode cell was filled with 100 mL of perchlorate solution using $Na_2SO_4$ as the supporting electrolyte. The perchlorate solution was fully mixed by a magnetic stirrer, and the pH value of the solution was measured by a pH meter, 0.1 M $H_2SO_4$ solution was added intermittently in order to maintain stability pH in the cathode cell. All experiments were conducted at an applied steady current.

## 3. Results and discussion

### 3.1. Characterizations of material

The microphotographs of Pd/BC and Re-Pd/BC were shown in Fig. 2(a) and (b). It could be observed that many spherical granules were adhered to the surface of Pd/BC in Fig. 2(a), and the similar micrograph of palladium particles immobilized on carbon material were reported by previous works [23,24]. In addition to spherical granules, the surface of Re-Pd/BC was found with many strip shape granules on the microphotographs (Fig. 2b). The presence of Pd on the surface of Pd/BC and Re on the surface of Re-Pd/BC was demonstrated by the EDX measurements respectively (Fig. 2). The XRD patterns of Pd/BC and Re-Pd/BC were shown in Fig. 3. The broad peaks locating at around 24.5° in all XRD patterns were attributable to graphene [25]. The strange Pd (1 1 1) peaks at around 40° could be seen for Pd/BC and Re-Pd/BC, and

two other Pd weak peaks located at 46° and 68°, it showed that the Pd content was low. The Re introduced to Pd/BC and did not cause strong change of Pd peaks, which could be explained by the fact that Pd and Re had similar covalent radii (0.128 nm) [26]. Furthermore, due to the dispersion of the Re component on the support or $ReO_4^-$ formation from the interaction of Re and the support, some of the Re might interact with the Pd, and an alloy or bimetallic cluster might be formed [27].

In Table 1, the surface area of BC was 794.62 $m^2$/g, the micropore volume was 0.054 $cm^3$/g and the mesopore volume was 0.389 $cm^3$/g of BC. When BC was modified by Re and Pd atomic, the surface area, the micropore and mesopore volume were observably decreased. The result demonstrated that BAC, Re and Pd could have a massive impact on porous structure of carbon material. The elemental compositions of the materials were investigated by XPS measurements. The results showed that Pd and Re were successfully loaded on the surface of Re-Pd/BC; the content of Pd was 1.9 at.% and the content of Re was 0.7 at.%. The high-resolutions of surface elementals were analyzed by the Gaussiantting program, and the results were shown in Fig. 4. According to the XPS spectrum of the C1s, it could be divided into four obvious peaks centering at 284.5, 285.1, 286.2 and 289.2 eV, respectively. The peak at 284.5 eV was related to $sp^2$ carbon, the peak at 285.1 eV could be attributed to combination of $sp^3$ carbon, the peak at 286.2 eV was corresponding to C-O- bonds and the peak at 289.2 eV was assignable to O=C-O- bonds [28–31]. The Pd XPS spectra of Pd/BC and Re-Pd/BC presented a doublet corresponding to Pd $3d_{5/2}$ and $3d_{3/2}$. The Pd $3d_{5/2}$ peak at 335.9 eV was attributed to $Pd^0$ (metallic palladium), the peak at 337.4 eV could be attributed to $Pd^{2+}$ (palladium oxide) [32,33]. XPS results indicated that Re-Pd/BC catalyst had two Re 4f peaks which appeared at 43.2 and 41.4 eV, respectively. The peak at 43.2 eV could be attributed to $Re^V$, and the peak at 41.4 eV could be attributed to $Re^I$ [10,34]. It was found that the O=C-O groups were disappeared on the Pd/BC and Re-Pd/BC after impregnation with 5 wt% Pd followed by pyrolysis at 523 K under $H_2$. This could be explained that Pd exhibited the high affinity for the carboxyl group on the surface of Pd/BC [35]. Moreover, Pd could be effectively catalyzed oxygen-containing group transformed by hydrogenation at pyrolysis under $H_2$ [36,37].

### 3.2. Perchlorate adsorption dynamic

The adsorption kinetics of perchlorate onto four kinds of material were shown in Fig. 5. Within the first 60 min, the perchlorate adsorption capacity reached 87.7%, 99.3%, 54.9% and 89.8 for CAC, BC, Re-Pd/CAC and Re-Pd/BC, respectively. The CAC modified by benzalkonium chloride could effectively improve perchlorate adsorption dynamics [3], due to quaternary ammonium groups doped on surface of
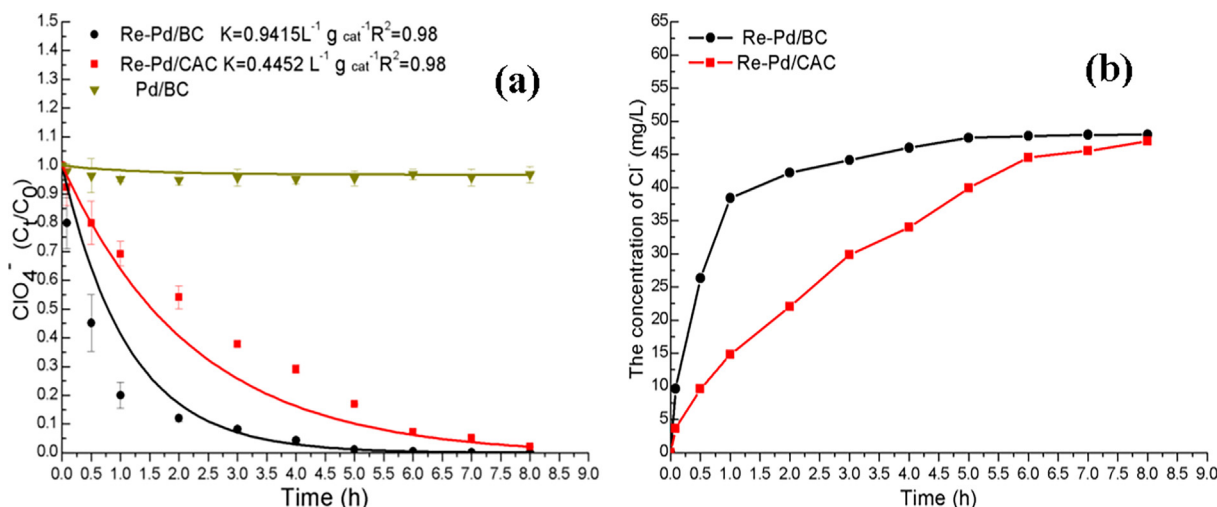


**Fig. 6.** (a) Electrochemical reduction for perchlorate (b) variation of chloridion concentration.

**Table 2**
The electrochemical reduction efficiency of various particle electrode for pollutant.

| Particle electrode | Pollutant | $C_0$ | Conditions | RE[a] (%) | References |
|---|---|---|---|---|---|
| Pd-In/Al$_2$O$_3$ | BrO$_3^-$ | 100 μg/L | 2 mM Na$_2$SO$_4$, pH = 7.0, CD[b] = 0.9 mA/cm$^2$ | 96.4 | [19] |
| Pd/GAC | Haloacetic acid | 120 μg/L | 200 mg/L Na$_2$SO$_4$, pH = 7.0, CD = 0.6 mA/cm$^2$ | 91 | [38] |
| Pd/AC | 4-chlorophenol | 300 mg/L | 5 g/L Na$_2$SO$_4$, pH = 7.0, CD = 0.8A | 100 | [39] |
| Fe-Pd/AC | 2-Chlorobiphenyl | 2 mg/L | pH = 6.5 | 90 | [40] |
| Re-Pd/BC | ClO$_4^-$ | 50 mg/L | 0.1 M Na$_2$SO$_4$, pH = 3.0, CD = 20 mA/cm$^2$ | 100 | This study |

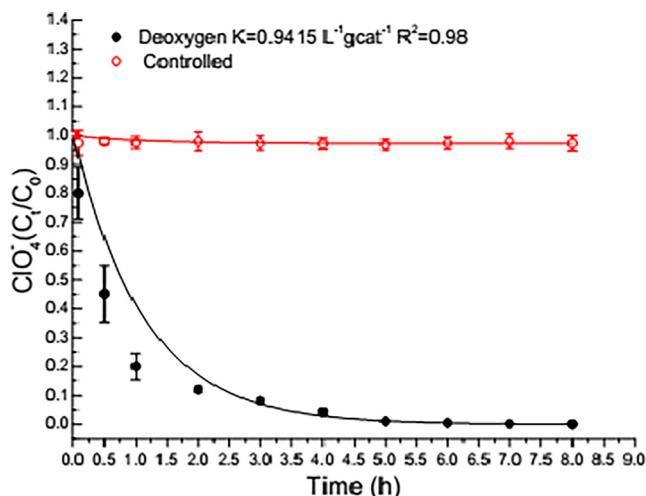RE[a] = Reduction efficiency.
CD[b] = Current density.



**Fig. 7.** Effect of aerobic on perchlorate electrochemical catalysis reduction.
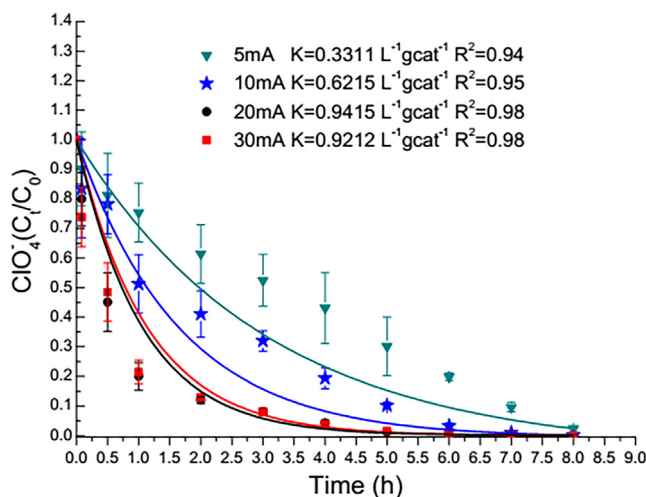


**Fig. 8.** Effect of current density on perchlorate electrochemical reduction.

carbon material. After modified by Re and Pd ions the carbon materials adsorption kinetics effectively decreased. The Re and Pd ions adhered to porosity structure and surface of carbon materials, leading to a markedly decreased in perchlorate transport transport pathway and adsorption sites [16]. The Re-Pd/BC had better adsorption kinetics compared with Re-Pd/CAC, it could facilitated ClO$_4^-$ adsorption and its subsequent reduction.

### 3.3. Efficient electrochemical catalysis reduction of perchlorate by Re-Pd/BC

The ClO$_4^-$ electrochemical reduction reaction of the cathode reactor, the solution concentration of ClO$_4^-$ was 50 mg/L; the solution pH was
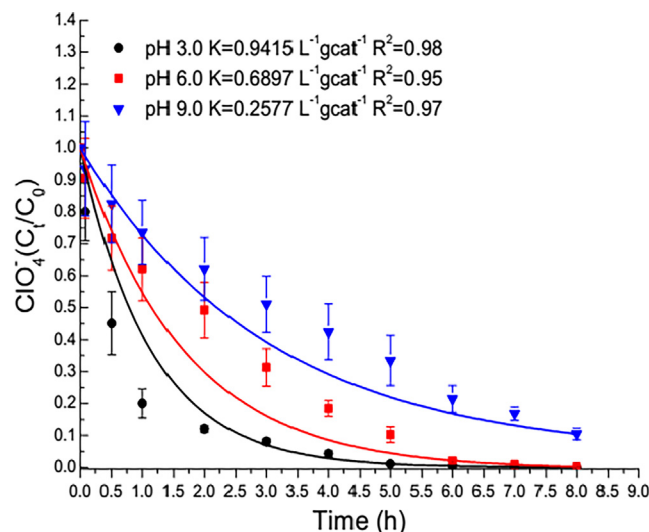


**Fig. 9.** Effect of solution pH on perchlorate electrochemical reduction.

3.0; the current density was 20 mA/cm$^2$, the reaction time was 8 h; nitrogen inlet was kept anaerobic environment; the Pd/BC, Re-Pd/BC and Re-Pd/CAC were used as the particle electrode. Comparison with the efficiency of ClO$_4^-$ electrochemical reduction by the Pd/BC, Re-Pd/BC and Re-Pd/CAC particle electrode and the result was presented in Fig. 6(a). In the first two hours, the concentration of ClO$_4^-$ was significantly decreased with the injection of continuous current sustained current injected. Subsequently, the concentration of ClO$_4^-$ gradually stabilized and the concentration of Cl$^-$ was remarkably increased, indicating that the ClO$_4^-$ could be effectively reduced by Re-Pd/BC and Re-Pd/CAC. However, the Pd/BC did not work for perchlorate reduction under the same conditions. Fig. 6(b) the loss of the corresponding value of 5–6% chloride with ClO$_4^-$ removal in the experiments of Re-Pd/BC and Re-Pd/CAC was due to the adsorption of some of ClO$_4^-$ and Cl$^-$ adsorbed by carbon materials. Perchlorate electrochemical reduction could be performed by using pseudo-first-order kinetic model to fit and the model equation was as follows:

$$\frac{d_x}{d_t} = -Kx \tag{2}$$

where $t$ was the reaction time (h), $x = x(t)$ was the ClO$_4^-$ concentrations (mg/L) at time of $t$, $\frac{d_x}{d_t}$ was the reaction rate, K was the reaction rate constant, $K > 0$ minus indicating the content of reactant was decreased. It could be noticed that the pseudo-first-order kinetic model was more appropriate for experiment data with higher correlation coefficients ($R^2 > 0.97$). The reaction rate constant K of Re-Pd/BC was 0.9415 L$^{-1}$ g$_{cat}$$^{-1}$, it was double than that of Re-Pd/CAC particles electrode (0.4452 L$^{-1}$ g$_{cat}$$^{-1}$). Compared with the reduction efficiency of pollutant, using particle electrode under the action of electrochemistry with the previous research (shown in Table 2), the performance of electrochemical reduction efficiency was better than many other particle electrode reported in the literature.
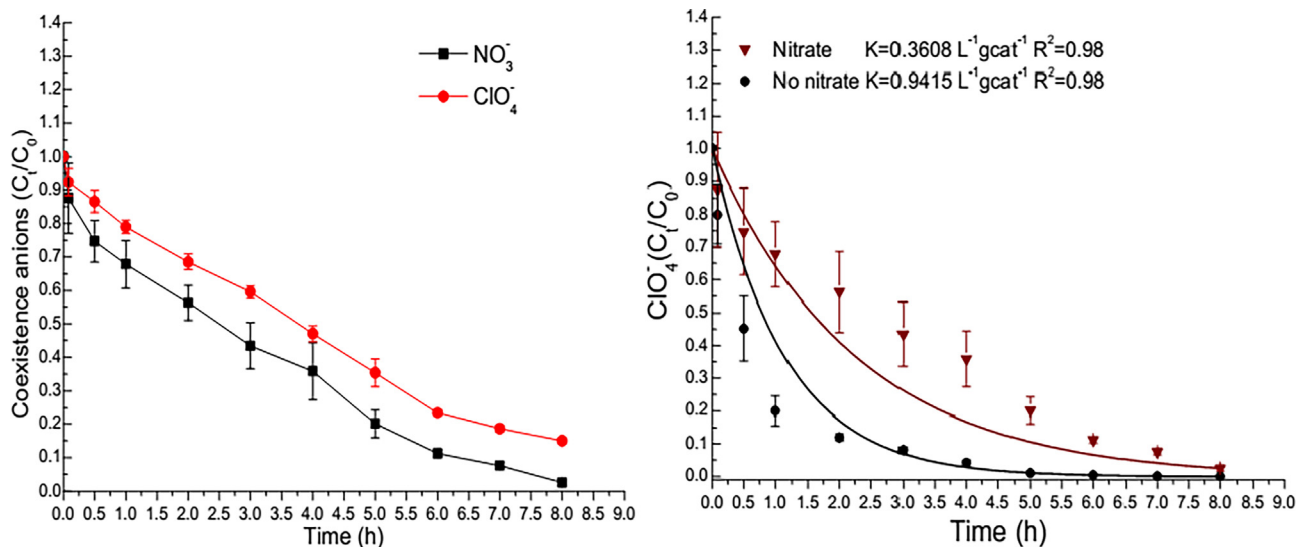
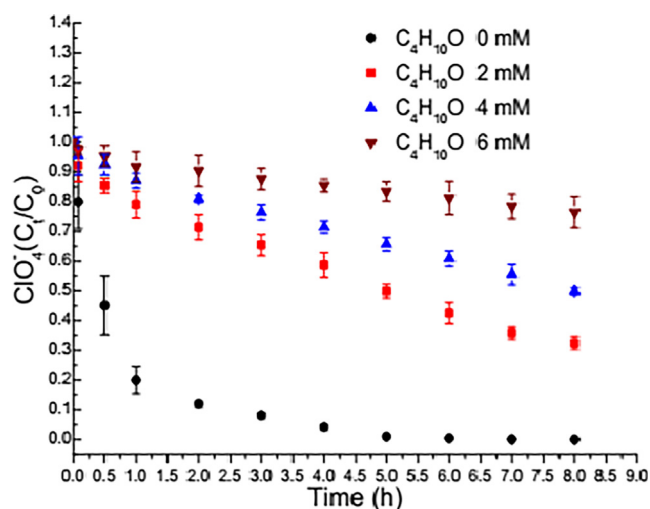Fig. 10. Effect of coexistence anion on perchlorate electrochemical reduction.



Fig. 11. Effect of $C_4H_{10}O$ concentrations on the electro-reduction of perchlorate.

### 3.4. Effect of oxygen on perchlorate reduction

The effect of aerobic and anaerobic environment on perchlorate electrochemical reduction for Re-Pd/BC was showed in Fig. 7. The Re-Pd/BC particles electrode had no effect on perchlorate electrochemical reduction, and there was no nitrogen inlet. This result was due to massive oxygen entering the solution of cathode reactor under the action of the magnetic stirrer, which could lead to $Re^V$ oxidized to $Re^{VII}$. Although the cathode could generate hydrogen through current and the $Re^{VII}$ could be reduced to $Re^V$ under the combined action of $Pd^0$, the reduction process was more complex than the oxidation process. At the same time, $Re^V$ oxidation rate was significantly higher than $Re^{VII}$ reduction rate, leading to the existence of Re in the form of $Re^{VII}$ on the surface of Re-Pd/BC. The entire perchlorate reduction cycle would be interrupted and lead to Re-Pd/BC particle electrode passivation.

### 3.5. Effect of current density on perchlorate catalysis reduction

The influence of surface electrode current density on the Re-Pd/BC was examined from 5 to 30 mA/cm². As shown in Fig. 8, the reduction rate markedly increased with current density (5–20 mA/cm²) and then remained constant at higher current of 30 mA/cm². Higher current

density would generate more available hydrogen and electrons [19], leading to higher perchlorate reduction efficiency. The similar reduction rate of Re-Pd/BC at 20 and 30 mA/cm² should be attributed to the limitation of active sites in the particle electrode, interfering with the electron transfer to perchlorate.

### 3.6. Effect of pH on perchlorate catalysis reduction

The Fig. 9 explored the influence of solution pH on the electro-reduction performance of Re-Pd/BC. Solution pH was the main factor affecting Re-Pd/BC in removing the perchlorate of the solution by electro-reduction at pH 3.0–9.0, and reduction rate markedly decreased with solution pH rising. The acidic environment significantly favored the generation of atomic H* [41] and Re-Pd bimetallic clusters could be partly dissociated in neutral and alkaline environment, which leaded to a significant decrease in the reduction rate.

### 3.7. Effect of coexisting ion on perchlorate catalysis reduction

The correlation research showed that common coexisting ions such as sulfate and chloride ion had little effect on perchlorate reduction, but nitrate ion had a significant effect [10,12,16]. Therefore, the influence of nitrate ion on the reduction of perchlorate by Re-Pd/BC was studied and the concentration of nitrate was 50 mg/L. The results, shown in Fig. 10, indicate that the nitrate concentration was about 20% of the initial concentration after 8 h reaction, and the perchlorate reduction rate constant decreased from 0.9451 to 0.3608 $L^{-1} g_{cat}^{-1}$, because the nitrate ion could be reduced to nitrogen or ammonium under Re-Pd bimetallic catalyzed [10]. Therefore, the presence of high concentration nitrate could be intensively competed with perchlorate available Pd-H* strong reducing agents, leading to a remarkably decreased in reduction rate.

### 3.8. Effect of atomic H* on perchlorate reduction

The research demonstrated that $C_4H_{10}O$ could effectively capture the H* atoms in the solution to form a 2-methyl-2propanol molecule [42]. In order to determine that H* played an important role in the perchlorate electrochemical reduction, batch experiments performed with the different stoichiometric concentrations of $C_4H_{10}O$ were performed. As presented in Fig. 11, the perchlorate reduction rate was remarkably decreased with the increasing of $C_4H_{10}O$ concentration, which indicated that H* played an important role in the whole
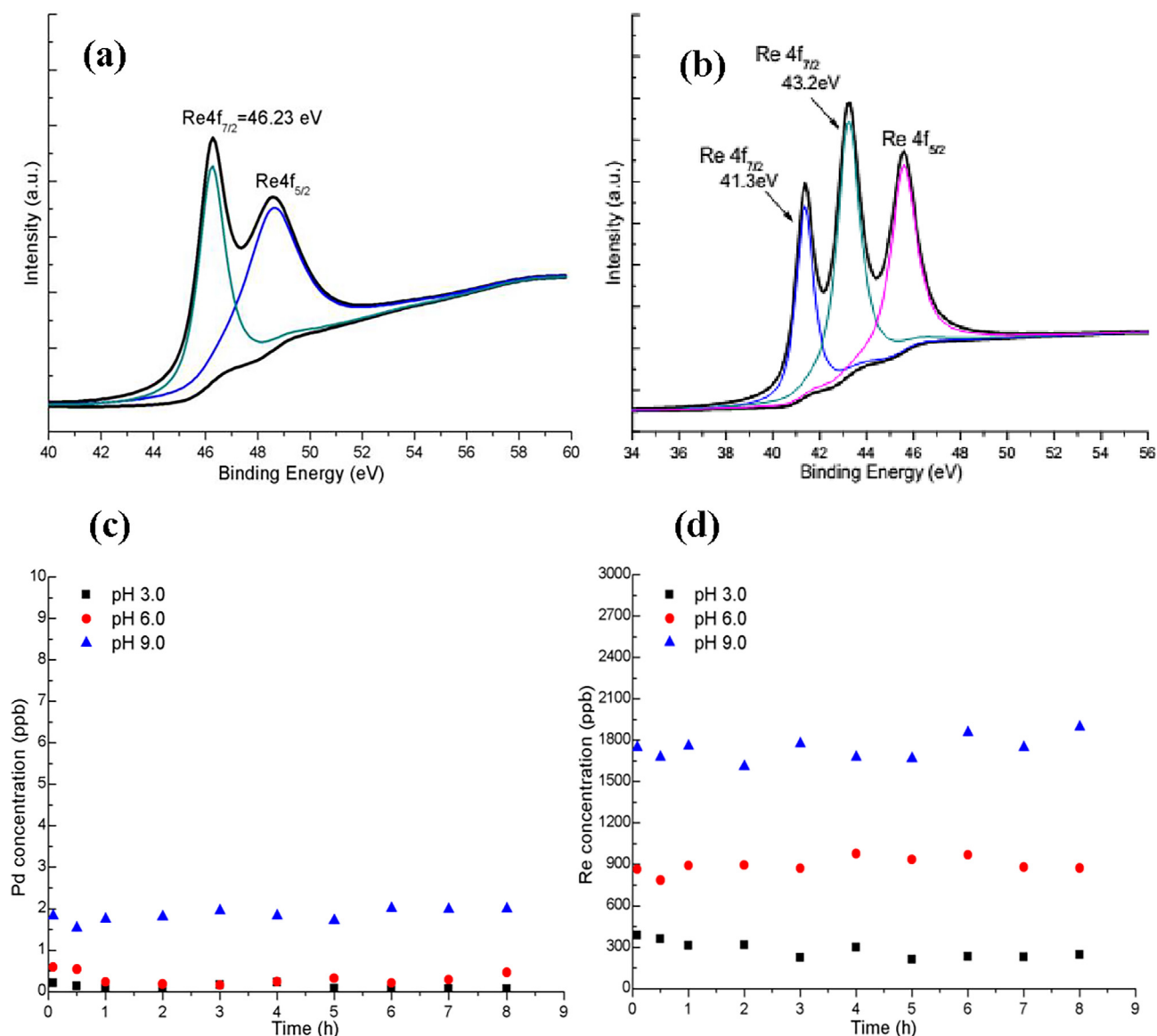
**Fig. 12.** The Re4f XPS spectral of (a) aerobic and (b) anaerobic after electrochemical reduction reaction, the concentration of (c) Pd and (d) Re at different pH.
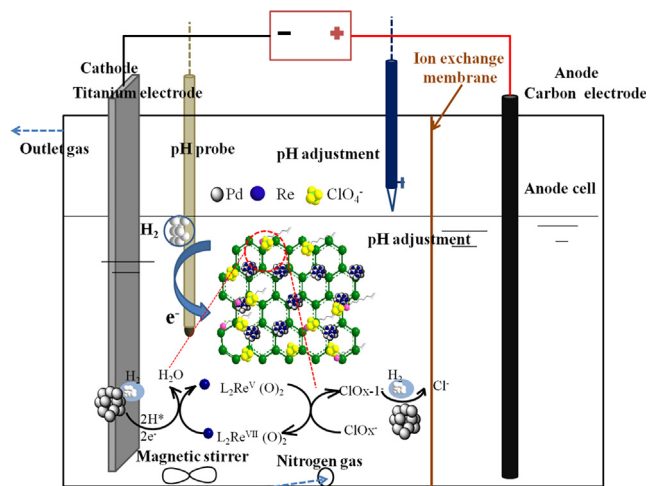


**Fig. 13.** Proposed electro-reduction mechanism of perchlorate by Re-Pd/BC.

perchlorate electrochemical reduction system.

### 3.9. Possible mechanisms

Firstly, the perchlorate was rapidly adsorbed to the surface of Re-Pd/BC particle electrode. With the application of a constant current on the titanium cathode (20 mA), the adhered water molecule was reduced to $H_2$. The Pd on the surface of Re-Pd/BC could effectively activate hydrogen to form $H^*$ atoms and bound $H^*$ atoms to form $Pd$-$H^*$ strong reducing agent [11]. As the Eqs. (3) and (4) shown $Ti + H_2O + e^- \rightarrow Ti$-$H^* + OH^-$ (3); $2Ti - H^* \rightarrow 2Ti + H_2$ (4), the concentration of hydroxide ion in the solution increased under titanium cathode action. In order to maintain the pH of the solution, hydrogen ions needed to be added from time to time. The perchlorate was adsorbed to the surface of particle electrode, and the same time two electrons were transferred to $ClO_4^-$ from $Re^V$ and formed $ClO_3^-$ and $Re^{VII}$. Moreover, $Re^{VII}$ was re-reduced to $Re^V$ by $Pd$-$H^*$ strong reducing agent, through repetition of the oxygen atom transfer cycle reaction (OAT) $ClO_3^-$ was rapidly transformed to $Cl^-$ [3]. In Fig. 6, in the first two hours of perchlorate electro-reduction, the concentration of $ClO_4^-$ was significantly decreased with injection of continuous current; subsequently the concentration of $ClO_4^-$

was gradually stabilized and the concentration of Cl⁻ was remarkably increased, indicating that the $ClO_4^-$ could be effectively reduced. The valence state of Re would had an important effect on perchlorate electrochemical reduction. As shown in Fig. 12 (a) when air was inlet, the valence state of Re as Re$^{VII}$ existed on the surface of Re-Pd/BC particle. Although there were production Pd-H* strong reducing agent by electrochemical reaction, reduction process of Re$^{VII}$ was more complex than oxidation process of Re$^V$. And the valence state of Re as Re$^{VII}$ existed on the surface of Re-Pd/BC particle, the whole oxygen atom transfer cycle reaction (OAT) was interrupted to cause the passivation of the Re-Pd/BC. In Fig. 12 (b), it was found the Re as Re$^I$ and Re$^V$ existed on the surface of Re-Pd/BC when nitrogen was inlet into solution after electrochemical reduction. When nitrogen was inlet the solution could effectively inhibit Re-Pd/BC passivation. The bimetallic cluster was the main reaction place for $ClO_4^-$ reduction, and the Re metal atoms could be effectively dissolved in alkaline solution, with the increase of pH, the Re-Pd bimetallic clusters were generally dissociated, leading to Re and Pd ions into solution [43,44]. In Fig. 12(c) and (d), the concentration of Re and Pd in solution was observably increased with the increase of pH. So the reduction rate constant obviously decreased with the increase of the solution pH. No other intermediate chloro-oxyanions (e.g., chlorite and chlorate) was detected in the whole electrochemical reduction process. The study showed that chlorite and chlorate kinetics were much lower than perchlorate, and the formation of chlorite and chlorate would be quickly reduced to chloride ion. The electrochemical reduction of perchlorate in the three-dimensional electrochemical reactor was shown in Fig. 13.

## 4. Conclusions

The research demonstrated that perchlorate could be effectively reduced to chloride using Re-Pd/BC as the particles electrode in the three-dimensional electrochemical reactor. Perchlorate ions could be rapidly adsorbed in the presence of benzalkonium chloride, facilitating its subsequent reduction on the Re-Pd/BC particle electrode. Superfluous oxygen in solution could lead to Re-Pd/BC deactivation; the reduction rate increased from 0.3311 to $0.9212\,L^{-1}\,g_{cat}^{-1}$; when the current density was from 5 to 30 mA/cm$^2$, the reduction rate decreased to $0.2577\,L^{-1}\,g_{cat}^{-1}$ when the solution pH was 9.0, the reduction rate decreased to $0.3608\,L^{-1}\,g_{cat}^{-1}$ in the presence of nitrate (50 mg/L). The perchlorate reduction rate constant reached to $0.9451\,L^{-1}\,g_{cat}^{-1}$ in optimization condition (pH 3.0, anerobic and current density 20 mA/cm$^2$). It was found that the existing form of Re and Pd on the surface of Re-Pd/BC, the number of atomic H* and current density played an important role in perchlorate electro-reduction process.

## Acknowledgements

## References

[1] Q. Fang, B. Chen, Adsorption of perchlorate onto raw and oxidized carbon nanotubes in aqueous solution, Carbon 50 (6) (2012) 2209–2219.

[2] J.K. Choe, M.H. Mehnert, J.S. Guest, T.J. Strathmann, C.J. Werth, Comparative assessment of the environmental sustainability of existing and emerging perchlorate treatment technologies for drinking water, Environ. Sci. Technol. 47 (9) (2013) 4644–4652.

[3] L. Ye, H. You, J. Yao, H. Su, Water treatment technologies for perchlorate: a review, Desalination 298 (2012) 1–12.

[4] D. Water, Regulatory Determination on Perchlorate, Environmental Protection Agency (EPA), 2011 7762-7767.

[5] Z. Ren, X. Xu, B. Gao, Q. Yue, W. Song, Integration of adsorption and direct bio-reduction of perchlorate on surface of cotton stalk based resin, J. Colloid Interface Sci. 459 (2015) 127–135.

[6] S. Baidas, B. Gao, X. Meng, Perchlorate removal by quaternary amine modified reed, J. Hazard. Mater. 189 (1–2) (2011) 54–61.

[7] Y. Xie, S. Li, F. Wang, G. Liu, Removal of perchlorate from aqueous solution using protonated cross-linked chitosan, Chem. Eng. J. 156 (1) (2010) 56–63.

[8] Y.-N. Kim, Y.-C. Lee, M. Choi, Complete degradation of perchlorate using Pd/N-doped activated carbon with adsorption/catalysis bifunctional roles, Carbon 65 (2013) 315–323.

[9] C. Zhang, C. Lai, G. Zeng, D. Huang, C. Yang, Y. Wang, et al., Efficacy of carbonaceous nanocomposites for sorbing ionizable antibiotic sulfamethazine from aqueous solution, Water Res. 95 (2016) 103–112.

[10] J. Liu, J.K. Choe, Z. Sasnow, C.J. Werth, T.J. Strathmann, Application of a Re–Pd bimetallic catalyst for treatment of perchlorate in waste ion-exchange regenerant brine, Water Res. 47 (1) (2013) 91–101.

[11] J. Liu, X. Chen, Y. Wang, T.J. Strathmann, C.J. Werth, Mechanism and mitigation of the decomposition of an oxorhenium complex-based heterogeneous catalyst for perchlorate reduction in water, Environ. Sci. Technol. 49 (21) (2015) 12932–12940.

[12] Y. Zhong, Q. Yang, X. Li, F. Yao, L. Xie, J. Zhao, et al., Electrochemically induced pitting corrosion of Ti anode: application to the indirect reduction of bromate, Chem. Eng. J. 289 (2016) 114–122.

[13] Z. Zhao, X. Peng, X. Liu, X. Sun, J. Shi, L. Han, et al., Efficient and stable electro-reduction of CO₂ to CH₄ on CuS nanosheet arrays, J. Mater. Chem. A 5 (38) (2017) 20239–20243.

[14] X. Liu, W. Xi, C. Li, X. Li, J. Shi, Y. Shen, et al., Nanoporous Zn-doped Co3O4 sheets with single-unit-cell-wide lateral surfaces for efficient oxygen evolution and water splitting, Nano Energy 44 (2018) 371–377.

[15] L.H. Lihan Zhang, Haoxuan Liu, Xijun Liu, Jun Luo, Potential-cycling synthesis of single platinum atoms for efficient hydrogen evolution in neutral media, Angew. Chem. Int. Ed. 56 (2017) 13694–13698.

[16] F. Yao, Y. Zhong, Q. Yang, D. Wang, F. Chen, J. Zhao, et al., Effective adsorption/electrocatalytic degradation of perchlorate using Pd/Pt supported on N-doped activated carbon fiber cathode, J. Hazard. Mater. 323 (2017) 602–610.

[17] I. Rhee, E.Y. Kim, B. Lee, K.-J. Paeng, Electrochemical reduction of perchlorate ion on porous carbon electrodes deposited with iron nanoparticles, J. Korean Electrochem. Soc. 18 (2) (2015) 81–85.

[18] R. Mao, X. Zhao, H. Lan, H. Liu, J. Qu, Graphene-modified Pd/C cathode and Pd/GAC particles for enhanced electrocatalytic removal of bromate in a continuous three-dimensional electrochemical reactor, Water Res. 77 (2015) 1–12.

[19] H. Lan, R. Mao, Y. Tong, Y. Liu, H. Liu, X. An, et al., Enhanced electroreductive removal of bromate by a supported Pd–In bimetallic catalyst: kinetics and mechanism investigation, Environ. Sci. Technol. 50 (21) (2016) 11872–11878.

[20] C.-X. Yuan, Y.-R. Fan, Z. Tao, H.-X. Guo, J.-X. Zhang, Y.-L. Wang, et al., A new electrochemical sensor of nitro aromatic compound based on three-dimensional porous Pt–Pd nanoparticles supported by graphene-multiwalled carbon nanotube composite, Biosens. Bioelectron. 58 (2014) 85–91.

[21] C. Zhang, C. Lai, G. Zeng, D. Huang, L. Tang, C. Yang, et al., Nanoporous Au-based chronocoulometric aptasensor for amplified detection of Pb2 + using DNAzyme modified with Au nanoparticles, Biosens. Bioelectron. 81 (2016) 61–67.

[22] Y. Zhai, B. Xu, Y. Zhu, R. Qing, C. Peng, T. Wang, et al., Nitrogen-doped porous carbon from Camellia oleifera shells with enhanced electrochemical performance, Mater. Sci. Eng., C 61 (2016) 449–456.

[23] C. Xu, L. Cheng, P. Shen, Y. Liu, Methanol and ethanol electrooxidation on Pt and Pd supported on carbon microspheres in alkaline media, Electrochem. Commun. 9 (5) (2007) 997–1001.

[24] T. Maiyalagan, K. Scott, Performance of carbon nanofiber supported Pd–Ni catalysts for electro-oxidation of ethanol in alkaline medium, J. Power Sources 195 (16) (2010) 5246–5251.

[25] Y.Z. Bibo Xu, Yun Zhu, Chuan Peng, Tengfei Wang, Chen Zhang, Caiting Liab, Guangming Zengab, The adsorption mechanisms of $ClO_4^-$ onto highly graphited and hydrophobic porous carbonaceous materials from biomass, RSC Adv. 6 (2016) 93975–93984.

[26] Z. Shao, C. Li, X. Di, Z. Xiao, C. Liang, Aqueous-phase hydrogenation of succinic acid to γ-butyrolactone and tetrahydrofuran over Pd/C, Re/C, and Pd–Re/C catalysts, Ind. Eng. Chem. Res. 53 (23) (2014) 9638–9645.

[27] Y. Li, H. Liu, L. Ma, D. He, Glycerol hydrogenolysis to propanediols over supported Pd–Re catalysts, RSC Adv. 4 (11) (2014) 5503.

[28] D. Bhattacharjya, H.-Y. Park, M.-S. Kim, H.-S. Choi, S.N. Inamdar, J.-S. Yu, Nitrogen-doped carbon nanoparticles by flame synthesis as anode material for rechargeable lithium-ion batteries, Langmuir 30 (1) (2014) 318–324.

[29] Wenzhong Shen, Z. Li, Y. Liu, Surface chemical functional groups modification of porous carbon, Recent Pat. Chem. Eng. 1 (2008) 27–40.

[30] X. Meng, Y. Zhong, Y. Sun, M.N. Banis, R. Li, X. Sun, Nitrogen-doped carbon nanotubes coated by atomic layer deposited SnO2 with controlled morphology and phase, Carbon 49 (4) (2011) 1133–1144.

[31] X. Li, X. Zhu, Y. Zhu, Z. Yuan, L. Si, Y. Qian, Porous nitrogen-doped carbon vegetable-sponges with enhanced lithium storage performance, Carbon 69 (2014) 515–524.

[32] Y. Wang, J. Yao, H. Li, D. Su, M. Antonietti, Highly selective hydrogenation of phenol and derivatives over a Pd@Carbon nitride catalyst in aqueous media, J. Am. Chem. Soc. 133 (8) (2011) 2362–2365.

[33] J.L. Zelong Li, Chungu Xia, Fuwei Li, Nitrogen-functionalized ordered mesoporous

carbons as multifunctional supports of ultrasmall pd nanoparticles for hydrogenation of phenol, ACS Catal. 3 (2013) 2440–2448.

[34] J.K. Choe, J.R. Shapley, T.J. Strathmann, C.J. Werth, Influence of rhenium speciation on the stability and activity of Re/Pd bimetal catalysts used for perchlorate reduction, Environ. Sci. Technol. 44 (2010) 4716–4721.

[35] B. An, H. Lee, S. Lee, S.-H. Lee, J.-W. Choi, Determining the selectivity of divalent metal cations for the carboxyl group of alginate hydrogel beads during competitive sorption, J. Hazard. Mater. 298 (2015) 11–18.

[36] H. Wang, J. Male, Y. Wang, Recent advances in hydrotreating of pyrolysis bio-oil and its oxygen-containing model compounds, ACS Catal. 3 (5) (2013) 1047–1070.

[37] L. Li, M. Chen, G. Huang, N. Yang, L. Zhang, H. Wang, et al., A green method to prepare Pd–Ag nanoparticles supported on reduced graphene oxide and their electrochemical catalysis of methanol and ethanol oxidation, J. Power Sources 263 (2014) 13–21.

[38] X. Zhao, A. Li, R. Mao, H. Liu, J. Qu, Electrochemical removal of haloacetic acids in a three-dimensional electrochemical reactor with Pd-GAC particles as fixed filler and Pd-modified carbon paper as cathode, Water Res. 51 (2014) 134–143.

[39] Y.Q. Cong, Z.C. Wu, Self-regeneration of activated carbon modified with palladium catalyst for electrochemical dechlorination, Chin. Chem. Lett. 18 (8) (2007) 1013–1016.

[40] H. Choi, S.R. Al-Abed, S. Agarwal, D.D. Dionysiou, Synthesis of reactive nano-Fe/Pd bimetallic system-impregnated activated carbon for the simultaneous adsorption and dechlorination of PCBs, Chem. Mater. 20 (11) (2008) 3649–3655.

[41] M.R. Gennero de Chialvo, A.C. Chialvo, Kinetics of hydrogen evolution reaction with Frumkinadsorption: re-examination of the Volmer-Heyrovsky and Volmer-Tafel routes, Electrochimica Acta 44 (44) (1998) 841–851.

[42] S.P. Mezyk, W.J. Cooper, K.P. Madden, D.M. Bartels, Free radical destruction of N-nitrosodimethylamine in water, Environ. Sci. Technol. 38 (2004) 3161–3167.

[43] V. Yatirajam, L. Kakkar, Separation of rhenium from molybdenum, vanadium, tungsten and some other elements by tribenzylamine-chloroform extraction from phosphoric acid, Anal. Chim. Acta 52 (3) (1970) 555–559.

[44] C. Li, W. Qu, A. Du, W.-J. Sun, Comprehensive study on extraction of rhenium with acetone in Re-Os isotopic dating, Rock Mineral Anal. 28 (3) (2009) 233–238.